A Novel *Bacillus thuringiensis* (PS149B1) Containing a Cry34Ab1/Cry35Ab1 Binary Toxin Specific for the Western Corn Rootworm *Diabrotica virgifera virgifera* LeConte Forms Ion Channels in Lipid Membranes

Luke Masson,*[,‡,§] George Schwab,[||] Alberto Mazza,[‡] Roland Brousseau,[‡,§] Lena Potvin,[‡] and Jean-Louis Schwartz*[,‡,§,⊥]

Biotechnology Research Institute, National Research Council, Montreal, Quebec, Canada H4P 2R2, Biocontrol Network and Groupe d'Étude des Protéines Membranaires and Department of Physiology, Faculty of Medicine, Université de Montréal, Montreal, Quebec, Canada H3C 3J7, and Warwick Consulting Group, Encinitas, California 92024

Received May 24, 2004; Revised Manuscript Received July 22, 2004

ABSTRACT: The binary *Bacillus thuringiensis* PS149B1 insecticidal crystal (Cry) protein is comprised of two components, Cry34Ab1, a 14-kDa protein, and Cry35Ab1, a 44-kDa protein, the combination of which forms a novel binary toxin active on western corn rootworm larvae. The permeabilizing behavior of the native binary toxin and its two individual components expressed as recombinant proteins was studied using calcein efflux determination in liposomes and by ion channel activity measurements in planar lipid bilayers (PLBs). Data obtained with solubilized native PS149B1 binary protein revealed it to be a pore-forming toxin that can permeabilize liposomes and form ion channels (∼300−900 pS) in PLBs at pH 5.5 but not pH 9.0. The 14-kDa component of the toxin also formed ion channels (∼15−300 pS) at pH 5.5 but did not insert easily in PLBs. While the 44-kDa moiety did seldomly form resolvable ion channels (∼15−750 pS) in PLBs, it did destabilize the membranes. It showed pH-dependent truncation to a stable 40-kDa protein. The purified 40-kDa truncated product formed channels (∼10−450 pS) in PLBs at pH 5.5. At that same pH, while a 3:1 molar mixture (14:44 kDa) of the individual components of the toxin induced channel activity that resembled that of the 14-kDa component alone, the 3:1 molar mixture of the 14-kDa component and 40-kDa truncated product induced channel activity (∼20−800 pS) similar to that of PS149B1 in planar lipid bilayers. We conclude that the overall membrane permeabilization process of Cry34Ab1/Cry35Ab1 is a result of ion channel formation.

The family of insecticidal toxins from the Gram-positive bacterium *Bacillus thuringiensis* is expressed as intracellular crystal (Cry)[1] proteins primarily during sporulation (*1*). The known toxin genes have been regrouped into 37 different gene classes (*2*; http://www.biols.susx.ac.uk/home/Neil_Crickmore/Bt/). These Cry proteins are toxic to a variety of lepidopteran, dipteran, and coleopteran larvae as well as some noninsect species (*1*, *3*) and have been used successfully as commercial sprayable products since the early 1950s. They are generally recognized as safe, environmentally friendly biopesticides (*1*, *4*). The Cry1 subclass represents a large group of single polypeptides in the 120−140-kDa range that, after proteolytic activation, are primarily toxic toward lepidopteran larvae. Other Cry proteins are also found as single polypeptides but in a variety of sizes ≤130 kDa. The first characterized insecticidal binary toxin was isolated from a mosquitocidal *Bacillus* strain, *Bacillus sphaericus* (*5*). This binary complex composed of a 42-kDa protein and a 52-kDa protein is capable of binding to mosquito midgut brush border membranes and forming ion channels in model membranes (*6*).

Due to the heavy usage of *B. thuringiensis*-based biopesticides in both forestry and agriculture, an understanding of the biochemical and physical properties of Cry toxins in relation to their molecular mode of action has assumed even greater importance both for safety assessment and for insect resistance management. When *B. thuringiensis* Cry protoxins are ingested by a susceptible insect, a series of events is triggered that include solubilization in the gut and modification by gut juice proteases, followed by the recognition of specific binding sites on the brush border epithelial cell membrane of susceptible insects (*1*). To date, it is generally accepted that, after binding to a docking receptor (*7*−*10*), the toxin undergoes a conformational change (*11*, *12*) and subsequently partitions into and permeabilizes the cell plasma membrane through pore formation (*13*−*17*). Cell death by a colloid osmotic lysis mechanism eventually ensues (*18*).

Recently, *B. thuringiensis* Berliner (strain PS149B1) (*19*) was isolated, and the purified crystal was found to be

* Corresponding authors: L.M. (tel, 514-496-6150; fax, 514-496-6213; e-mail, luke.masson@nrc.ca) and J.-L.S. (tel, 514-343-6364; fax, 514-343-6631; e-mail, jean-louis.schwartz@umontreal.ca).

‡ National Research Council.

§ Biocontrol Network, Université de Montréal.

|| Warwick Consulting Group (formerly Dow AgroSciences, LLC, San Diego, CA 92121).

⊥ Groupe d'Étude des Protéines Membranaires and Department of Physiology, Faculty of Medicine, Université de Montréal.

[1] Abbreviations: Cry, crystal; PLBs, planar lipid bilayers; PC, phosphatidylcholine; PE, phosphatidylethanolamine; PS, phosphatidylserine; R_H, hydrodynamic radius; LUVs, large unilamellar vesicles; kDa, kilodaltons; pS, picosiemens.

10.1021/bi048946z CCC: $27.50
Published on Web 08/31/2004

composed of two novel Cry proteins, a 14-kDa (Cry34Ab1) and a 44-kDa protein (Cry35Ab1). Further investigation using the cloned gene products revealed that when the two proteins were combined, the resulting binary toxin was toxic toward the western corn rootworm (*Diabrotica virgifera virgifera* LeConte, Coleoptera), a major pest of maize (*20*). The 14-kDa Cry34Ab1 protein alone showed activity against southern corn rootworm, *Diabrotica undecimpunctata howardi* Barber, but was clearly synergized by the 44-kDa protein, indicating that both proteins are required for maximal insecticidal activity (*20*).

The two PS149B1 protein sequences do not share similarity with any of the known Cry proteins although there is some evolutionary relatedness between the larger Cry35Ab1 protein and the 42-kDa and 51-kDa dipteran-active toxins from *B. sphaericus* (*19*, *21*). While atomic structures have been determined for four Cry toxins, i.e., Cry3Bb1, Cry3A1, Cry2Aa, and Cry1Aa (*22*−*25*), and although Cry3A, Cry3B, and Cry2A only share a low (∼36%) amino acid similarity with Cry1Aa, all four structures display a common globular shape composed of three distinct domains involved mainly in membrane insertion and pore formation (domain I) and receptor binding (domains II and III).

This study was designed to explore the mode of action of the novel *B. thuringiensis* (PS149B1) binary crystal to ascertain whether the solubilized crystal forms pores in phospholipid membranes like other known Cry toxins. To do so, we investigated the membrane-permeabilizing properties of the full binary toxin and its individual components reconstituted into liposomes and planar lipid bilayers. We show for the first time that the binary toxin and its individual components are capable of permeabilizing phospholipid vesicles and that the native toxin or a mixture of its components forms channels in planar lipid bilayers. The toxicity of the binary toxin may therefore result from the formation of lytic pores in target cell membranes.

EXPERIMENTAL PROCEDURES

Chemicals and Solutions. Lipids used were phosphatidylcholine (PC), phosphatidylethanolamine (PE), and phosphatidylserine (PS) from Avanti Polar Lipids (Alabaster, AL) and cholesterol from Sigma (St. Louis, MO). All were at least 99% pure by TLC, according to the manufacturer. Calcein was from Molecular Probes (Eugene, OR), EDTA from International Biotechnologies Inc. (New Haven, CT), Sephadex-G50 from Pharmacia Fine Chemicals AB (Uppsala, Sweden), and Triton X-100 from Mallinckrodt (Paris, KY). For vesicle preparation and permeabilization experiments, the following solutions were used: solution A, 20 mM KCl, 5 mM EDTA, and 100 mM phthalate, pH 5.5; solution B, 140 mM KCl, 5 mM EDTA, and 100 mM phthalate, pH 5.5, 6.5, or 11.0. The PLB chamber solution (PLB solution) contained 150 mM KCl, 1 mM $CaCl_2$, and 10 mM Tris-HCl, pH 5.5, or 10 mM Tris-base, pH 9.0, depending on the experiments. Channel ionic selectivity was tested at pH 5.5 under asymmetrical conditions using a modified PLB solution containing 450 mM KCl in the cis chamber and the regular 150 mM KCl PLB solution in the trans chamber of the lipid bilayer apparatus.

Bacterial Strains and Toxin Preparation. Production and purification of the *B. thuringiensis* strain PS149B1 binary crystal and its two cloned recombinant gene products, the 14-kDa Cry34Ab1 (MR1256) and the 44-kDa Cry35Ab1 (MR1253), as crystal suspensions have been described previously (*26*). The white PS149B1 binary crystals and the recombinant inclusions were stored in distilled water at 4 °C. Solubilized toxin preparations were prepared as follows: aliquots of the crystal/inclusion body suspension were solubilized in 50 mM citrate, pH 3.0, for 1 h at 37 °C. Undissolved material was removed by centrifugation at 10000*g* for 10 min and the supernatant collected and recentrifuged at 200000*g* for 1−2 h to remove lipids. The supernatant was dialyzed for 16 h in prepared dialysis tubing (8-kDa MWCO) against three changes of deionized water at 4 °C. The precipitated protein was harvested by centrifugation in a 15 mL Corex centrifuge tube and the pellet resuspended and washed twice in 1.5 mL of distilled H_2O by spinning 30 s in a microfuge. All protein concentrations were determined either by the protein−dye method of Bradford (1976) using bovine serum albumin as a standard or as dry weight after 80% acetone precipitation and lyophilization. Recombinant Cry35Ab1 (44-kDa protein from MR1253) inclusions were found to be approximately 95% pure as compared to native PS149B1 crystals as estimated by SDS−PAGE gels. No addition of protease inhibitors to binary crystal stocks was attempted since some degradation of the 44-kDa to the 40-kDa form was generally present in the crystal form as observed by direct solubilization by boiling in sodium dodecyl sulfate containing protein gel loading buffer. To purify its 40-kDa truncated product, the recombinant 44-kDa protein was solubilized in 50 mM Bis-Tris at pH 6.0 for 60 min, passed through a 0.2 μm filter, and centrifuged at 200000*g* for 1−2 h to remove lipids. After verification of the 44- to 40-kDa conversion by SDS−PAGE, the supernatant was dialyzed against water, as described above, to precipitate the protein.

Light Scattering Measurements. To determine the hydrodynamic radius (R_H) of the purified recombinant toxin molecules, a dynamic light scattering apparatus (DynaPro-801; Protein Solutions, Inc., Charlottesville, VA) was used. The determined radii were fitted to a monomodal Gaussian distribution using Dynamics software (version 3.0; Protein Solutions Inc.) to ascertain whether the protein species in solution is monodisperse (i.e., a single species) and to provide an estimate of the molecular mass of the protein under study. If the sample has more than one molecular species (i.e., a mixture of monomers, dimers, etc.), then the data are fitted to a bimodal size distribution to ascertain whether a second discrete species can be determined. Toxin solutions, prepared in doubly distilled water, under the following 50 mM buffer conditions, (a) citrate, pH 3.0, (b) phthalate, pH 2.5, (c) phthalate, pH 5.0, (d) MES, pH 5.5, (e) Bis-Tris, pH 6.0, (f) CAPS, pH 11.5, and (g) CAPS, pH 11.5, 150 mM NaCl, and 10 mM DTT, were adjusted to approximately 0.7 mg/mL with the appropriate buffer after being passed through a 100 nm filter. The different toxin solutions (20 μL) were placed into the quartz cuvette and 7−12 readings per sample were recorded.

Calcein Release from Unilamellar Vesicles. A 4:1 (w/w) mixture of PC and PS in chloroform was dried under nitrogen and hydrated at a concentration of 9.1 g/L in a solution containing 80 mM calcein (pH 5.5 adjusted with KOH). It was subjected to 10 cycles of freezing and thawing in a dry

ice/ethanol bath and boiling water to form multilamellar liposomes. Large unilamellar vesicles (LUVs) loaded with calcein were then prepared in solution A, using an extrusion technique (*27*) through 0.1 μm polycarbonate filters (Nucleopore; Costar, Cambridge, MA) mounted in a dual, 250 μL syringe miniextruder apparatus (Avestin, Ottawa, Ontario, Canada). The untrapped dye was removed by exclusion chromatography using a column filled with Sephadex G-50 fine gel swollen in isotonic buffer (*28*). The permeabilizing activity of the proteins at doses between 20 and 200 μg/mL was evaluated by measuring the release of calcein from the LUVs (*6*) using a spectrofluorometer (Sciencetech, London, Ontario, Canada) equipped with a R928 photomultiplier detector. Aliquots of washed LUVs were placed in solution B (total volume of 1.5 mL) in a 1 cm light path, stirred plastic cuvette. The final lipid concentration was around 2 mM. After toxin addition, the time course of calcein release was recorded as an increase in the fluorescence emitted at 510 nm with the excitation set at 495 nm (5 nm slit setting). Such a fluorescence signal results from the dequenching of the dye when it is released from the LUVs and diluted in the external medium. Experiments were conducted at room temperature and pH 5.5, 6.5, or 11. At the end of each experiment, the maximal value of calcein release was assessed by addition of 1% Triton X-100. Spontaneous release of calcein was usually quite negligible (less than 3%); if present, it was subtracted from the *B. thuringiensis* protein-induced release. Fluorescence data were smoothed using a running average protocol over 10 successive samples, and the resulting curves were fitted with cubic polynomial functions.

Planar Lipid Bilayers. PLBs (*29*) were formed from a 7:2:1 (w/w) lipid mixture (25 mg/mL final concentration in decane) of PE, PC, and cholesterol. The bilayer was painted, using disposable glass rods made from prepulled, sealed-tip Pasteur pipets, across a 250 μm orifice separating two small volume chambers (5 mL trans, 3 mL cis) and pretreated with the above lipid mixture dissolved in decane. Membrane thinning was monitored by visual observation through a binocular dissection microscope and was assayed electrically. Typical membrane capacitance values ranged between 150 and 200 pF. Under the conditions used in this study, membranes remained stable for hours. At the beginning of each experimental session, they were tested for 15−20 min, at various holding voltages, for the absence of channel-like activity. Protein incorporation was promoted by stirring the solution in the cis chamber using a magnetic stir bar and by applying holding voltages between ±100 mV. Channel activity was monitored by step changes in the current recorded during holding test voltages applied to the PLBs. All experiments were performed at room temperature (20−22 °C).

Standard incorporation protocols were used for the full toxin or its individual components (*14*); i.e., 15−60 μg aliquots of the proteins prepared in a 50 mM sodium citrate, pH 3.0, stock solution were added to the cis chamber, after bilayer formation, to reach final concentrations of 5−20 μg/mL. In some experiments, the toxin was first reconstituted into liposomes (*13*). A 4:1 (w/w) mixture of PC and PS in chloroform was dried under nitrogen and hydrated at a concentration of 9.1 g/L in a buffer solution containing 150 mM sodium citrate, 0.1 mM EDTA, 10 mM Bis-Tris, pH 3.0, and 0.1 g/L *B. thuringiensis* protein. Following a 5 min vortexing period, the mixture was freeze−thawed 10 times in a dry ice/ethanol bath and boiling water. The lipid−protein mixture was then used to prepare LUVs by extrusion as described above. After 10−15 min following membrane formation, 30 μL of proteoliposomes was added to the 3 mL cis chamber. Vesicle fusion to the PLB was promoted by the establishment of a transbilayer osmotic gradient by addition of 160 mM urea in the cis chamber, by the presence of 10 mM calcium ions, and by stirring (*30*).

In experiments designed to investigate the interaction between the individual components of the PS149B1 toxin, the following protocol was used: after addition to the cis chamber of a 15−60 μg aliquot of the first component to be tested, channel activity was recorded. A 15−60 μg aliquot of the second component was then injected in the same chamber, and recording was resumed. PLB experiments were also conducted on a 1:1 (w/w) mixture of the two components either preincubated overnight or premixed for 1 h before addition to the cis chamber. This ratio was found to produce a higher lethality in bioassays with western corn rootworm larvae than either toxin alone (*20*).

Electrical connections between the chambers and the recording instrumentation were made with Ag/AgCl electrodes and agar salt bridges (2% in 0.2 M KCl, 1 mM EDTA). Single channel currents were recorded with an Axopatch-1D patch-clamp amplifier (Axon Instruments, Foster City, CA), filtered at 5 kHz, displayed on an oscilloscope (Kikusui 5020A, Tokyo, Japan), pulse-code modulated (CRC VR-100A; Instrutech Corp., Great Neck, NY), and stored on videotape. Currents were played back, filtered at 600 Hz through an analogue 8-pole Bessel filter (Model 902; Frequency Devices, Haverhill, MA), and digitized at a 2.5 kHz sampling frequency using a Labmaster TL-125 interface (Axon Instruments) and Axotape version 1.2.01 software (Axon Instruments). Analysis was performed on a personal computer using pClamp version 6.0 software (Axon Instruments).

For each applied voltage, current amplitudes were measured on the recorded traces. For some voltages, current amplitude histograms were generated. Channel conductances were estimated from the slopes of the linear regressions on the data points of the current−voltage relations. Applied voltages are defined with respect to the trans chamber that was held at virtual ground. Positive currents (i.e., currents flowing through the PLBs from the cis chamber to the trans chamber) are shown as upward deflections. The direction of current flow corresponds to positive charge movement.

RESULTS

Liposome Permeabilization by the PS149B1 Binary Crystal and Its Components. The purified native PS149B1 crystal and the recombinant 14k-Da and 44-kDa proteins (Figure 1) were assessed for liposome permeabilization by monitoring the calcein efflux from phospholipid vesicles. This assay detects the formation of large pores, ionic or not, or simply membrane destabilization or defects. Vesicle permeabilization by the toxin results in the leakage of calcein, a 622-Da molecule with a hydrated Stokes radius of 0.75 nm. As shown in Figure 2, calcein efflux from preloaded LUVs was induced by the addition of the full PS149B1 solubilized

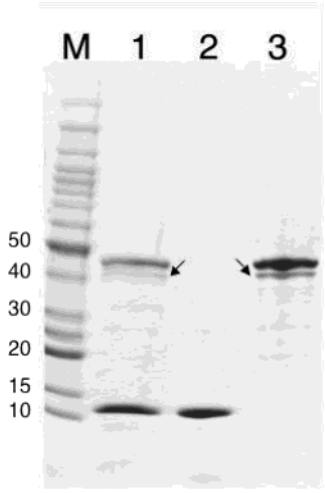

FIGURE 1: SDS−PAGE of purified native PS149B1 binary toxin and the individual recombinant gene products derived from strain PS149B1. Approximately 2 μg of protein per lane was loaded onto a 4−15% gradient SDS−PAGE gel. Key: M, molecular mass markers (kDa); lane 1, PS149B1 crystal; lane 2, 14-kDa protein from Cry34Ab1; lane 3, 44-kDa protein from Cry35Ab1. The 40-kDa truncated product of the 44-kDa protein is indicated with arrows.

crystal (Figure 2A), the 14-kDa component (Figure 2B), and the 44-kDa component (Figure 2C). Efficient experimental conditions were difficult to establish because of the adverse effect of several of the buffer solutions on liposome integrity. This was particularly true for the phthalate buffer. Under optimal conditions, the amount of calcein leakage induced by exposure to the PS149B1 toxin individual components was small (5−7% of the Triton X-100 response at 200 μg/mL toxin dose) compared to that caused by a different *B. thuringiensis* toxin, Cry1Aa (approximately 30% of the Triton X-100 response at up to 200 μg/mL toxin dose; data not shown).

PS149B1 Binary Toxin Activity in Planar Lipid Bilayers. At alkaline pH (i.e., pH 9.0), the PS149B1 binary toxin partitioned poorly in planar lipid bilayers. However, under acidic pH conditions (i.e., pH 5.5), addition of solubilized PS149B1 crystals to the PLB bath resulted in ion channel formation with a 62% success rate (Table 2). The trace in Figure 3A shows the currents recorded at two opposite voltages at which similar ion channel activity was observed with clear channel openings and closings. As illustrated by the current−voltage relation curves obtained from seven separate experiments (Figure 3B), the channel conductance of the PS149B1 toxin was ohmic (i.e., recorded currents were proportional to the applied voltages) with a range spanning a large spectrum from 310 to 920 pS. The channels usually tended to stay open for long periods of time, and in some experiments, flickering activity was observed. During the course of the experiments, more and more current levels were observed, suggesting that either more channels became active or more proteins partitioned into the membrane, or both. Some channels displayed voltage dependence, i.e., had opening probabilities that depended on the applied voltage. Kinetic analysis of the channels was difficult to perform due to the multichannel nature of the recordings. However, in one experiment in which only one channel was active, it was found that the channel behavior could be described by one

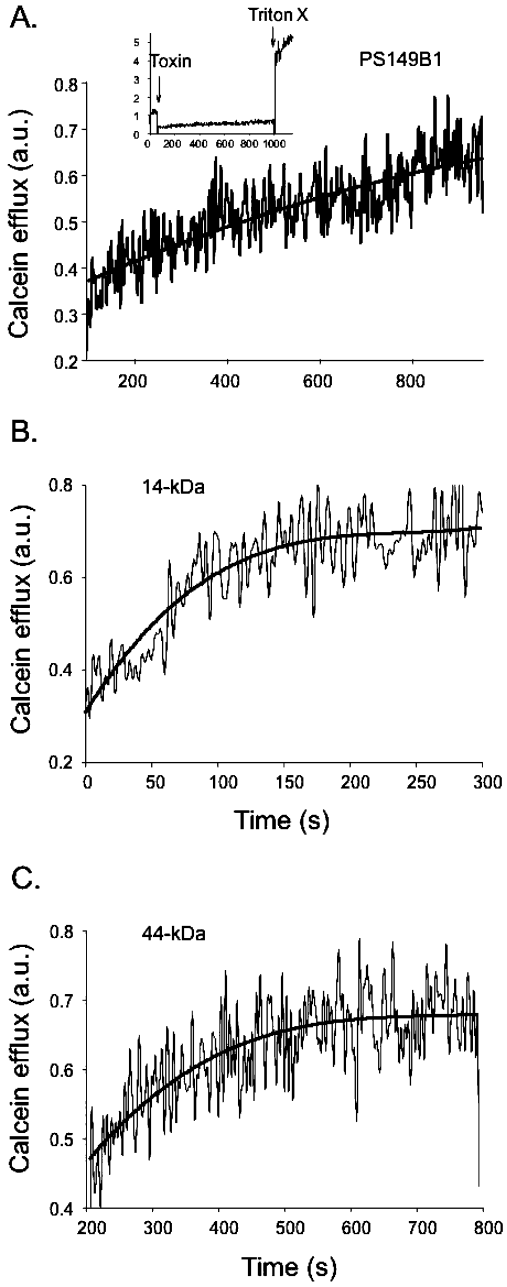

FIGURE 2: Typical calcein release from large unilamellar vesicles (LUVs) exposed to 200 μg/mL full PS149B1 *B. thuringiensis* toxin in one experiment conducted at pH 5.5 (A), to 20 μg/mL 14-kDa moiety in another experiment at pH 5.5 (B), and to 100 μg/mL 44-kDa moiety in another experiment at pH 5.5 (C). Each record is representative of three different experiments conducted under identical conditions. At the time corresponding to the beginning of each trace, 20−200 μg/mL protein was added to a 1 cm stirred quartz cuvette containing around 2 mM washed LUVs in a total volume of 1.5 mL of solution B. The pH was adjusted to 5.5, 6.5, or 11.0. LUVs were made of a mixture of the phospholipids PC: PS (4:1 w/w). Calcein fluorescence was determined with a spectrofluorometer at 495 nm excitation and 510 nm emission wavelengths. Cubic polynomial regression lines are shown as continuous heavy lines through experimental data corrected for the small calcein leakage (less than 3%) in the absence of the proteins and smoothed by a running average protocol over 10 successive data points (continuous light lines). The insert in (A) illustrates the time course of a complete experiment where total calcein release was achieved by the addition of 1% Triton X-100 at the end of the experiment.

open state (mean open time of 12.4 ms) and two closed states (mean closed times of 1.3 and 3.3 ms).

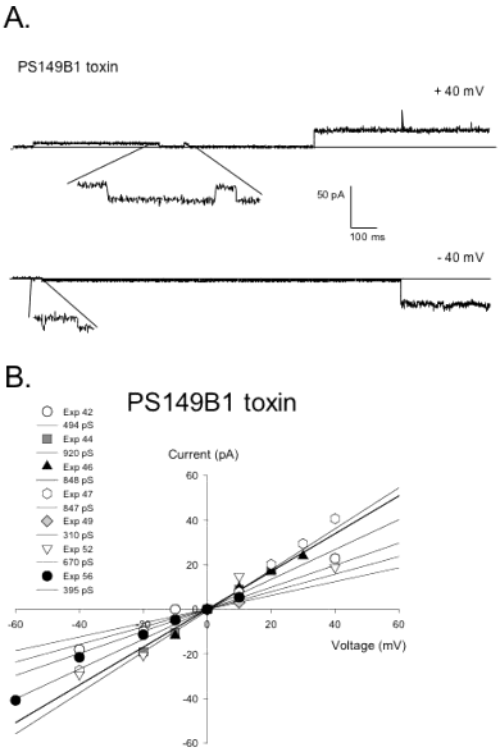

FIGURE 3: (A) Typical single channel currents observed in PLBs at pH 5.5 with native PS149B1 binary toxin. The final protein concentration ranged from 5 to 20 μg/mL. Well-resolved current steps are illustrated by the expanded time scale (by a factor of ~4) and amplitude scale (by a factor of ~5) traces shown below each main trace. The single channel recordings were made at ±40 mV holding voltages as shown over each main current trace. Horizontal continuous lines indicate the estimated closed state of the channels. (B) Current−voltage relations of the channels formed by the PS149B1 *B. thuringiensis* toxin in PLBs at pH 5.5. For each of the seven experiments illustrated in this figure, data points are shown with different symbols (see legend on the upper left quarter of the graph). Linear regression lines to the data points are also shown, from the slopes of which the conductances were derived. Vertical axis: channel current (pA). Horizontal axis: applied voltage (mV).

Protein Stability. Initial attempts in assessing membrane permeabilization activity of the purified recombinant 44-kDa protein under conditions typically used for other Cry toxins (*11*, *14*, *15*) resulted in a low success rate. Membrane currents were seldom observed and often did not display clean, steplike patterns associated with ion channel activity. It was observed, however, that solubilization of the binary crystal in citrate buffer, pH 3.0, resulted in the appearance of a faint 40-kDa protein band (Figure 1, lane 1). This minor band could also be found with the recombinant 44-kDa protein (Figure 1, lane 3; Figure 4, lane 1), suggesting that it was a truncated product of the 44-kDa component. N-Terminal sequencing showed an intact N-terminus, suggesting that cleavage occurred at the C-terminal end (Yong Gao, Dow AgroSciences, personal communication). To determine the effect of pH on truncation of the 44-kDa protein, purified water-precipitated 44-kDa protein was solubilized for 2 h in various buffers with pH ranging from 3.0 to 11.5. As shown in Figure 4, the 44-kDa protein underwent a stable conversion to the 40-kDa species with the optimum pH being between 5.5 and 6. This observation permitted the use of a simple method for the subsequent purification of a stable 40-kDa protein. To confirm whether this conversion was due to crystal-associated proteases, a serine protease (bovine trypsin) or a cysteine protease (papain) was added to solubilized 44-kDa protein. The results showed that trypsin and papain rapidly degraded the protein to small peptides (data not shown), suggesting that some as yet unidentified protease may be responsible for the conversion of the 44-kDa protein to the 40-kDa fragment.

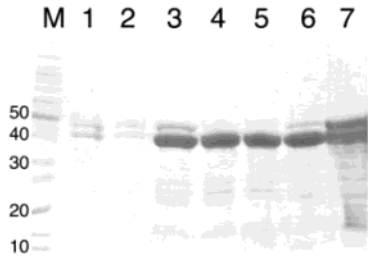

FIGURE 4: Effect of pH on the activation of the recombinant 44-kDa protein. Approximately 100 μg of recombinant Cry35Ab1 was solubilized in 50 mM citrate buffer at pH 3.0 and rapidly diluted into buffers of varying pH. All toxin solutions were allowed to stand at room temperature for 4 h before being loaded onto a 4−15% gradient SDS−PAGE gel. Key: M, molecular mass markers (kDa); lane 1, 50 mM citrate, pH 3.0; lane 2, 50 mM citrate, pH 3.5; lane 3, 50 mM citrate, pH 4.0; lane 4, 50 mM Bis-Tris, pH 5.5; lane 5, 50 mM Bis-Tris, pH 6.0; lane 6, 50 mM HEPES, pH 7.4; lane 7, 50 mM carbonate, pH 10.0. A smaller amount of protein was added to lanes 1 and 2 to clearly distinguish the 44-kDa protein from the 40-kDa truncated product.

Table 1: Determination of Hydrodynamic Radii and Aggregation States of Purified Recombinant Cry34Ab1 and Cry35Ab1 Proteins

purified toxin[a]	hydrodynamic radius (nm)	estimated molecular mass (kDa)
recombinant 14-kDa protein	2.0 (0.01)[b]	14.5 (0.13)
40-kDa truncated product of recombinant 44-kDa protein	3.2 (0.1)	47.3 (3.8)
recombinant 44-kDa protein	28.2 (9.5)	21624.4 (12977.1)

[a] All toxins were purified, water-precipitated proteins solubilized in 50 mM Bis-Tris, pH 5.5. [b] Numbers in parentheses = standard error.

Dynamic light scattering was used to assess the aggregative state of the purified 14-, 40-, and 44-kDa recombinant proteins. Dissolution of the 14-kDa protein in acidic pH buffers, citrate, phthalate, MES, and Bis-Tris, all resulted in a stable monomeric form whereas the 44-kDa protein was only found in a large multimeric state (>50-mer) in all buffers assayed (data not shown). The light scattering results for all three proteins dissolved in 50 mM Bis-Tris at pH 6.0 are shown in Table 1. The calculated hydrodynamic radius for each preparation showed the 14- and the 40-kDa proteins to be in a monomeric state and the 44-kDa protein to be highly aggregated. The calculated molecular mass of the 40-kDa truncated product was found to be slightly higher (i.e., 47 kDa) but within the 20% error range of the DynaPro apparatus. This overestimation may occur when very low levels of multimers may be present. On the basis of these results, 50 mM Bis-Tris, pH 5.5−6.0, was utilized for all further permeabilization experiments.

Activity of the PS149B1 Recombinant Proteins in Planar Lipid Bilayers. Like PS149B1, the recombinant components of the crystal did not form clearly resolved ion channels in PLBs at alkaline pH. However, they were capable of destabilizing the bilayers, i.e., of interacting in an unstructured way with membrane phospholipids, as evidenced by

Table 2: Channel Formation and Characteristics of PS149B1 and the Recombinant Proteins Cry34Ab1 and Cry35Ab1 at pH 5.5

	protein source				
	PS149B1 binary toxin	Cry34Ab1 component (14 kDa)	Cry35Ab1 component (44 kDa)	Cry35Ab1 (40-kDa fragment)	3:1 molar mixture (14:40 kDa)
conductance[a] (pS)	310−920	15−300	15−750	8−430	20−765
success rate (%)[b]	62 (26/42)	15 (6/40)	18 (7/39)	32 (6/19)	45 (5/11)
ease of partition[c]	+++	+	+	++	++
full channel closure (%)[d]	40	67	50	33	9

[a] Determined either as conductance at full closure (when channel current returned to zero), as conductance to baseline (when at least one channel remained always open), or as conductance from analysis of all current steps. [b] % success rate = 100(number of successful integrations producing measurable current steps)/(total number of experiments) [these numbers are given in parentheses]. [c] Time to first detectable current step after protein addition to the PLB bath: +++, less than 15 min; ++, between 15 and 30 min; +, more than 30 min. [d] Percentage of experiments in which the channel current returned to zero within the duration of the recordings.

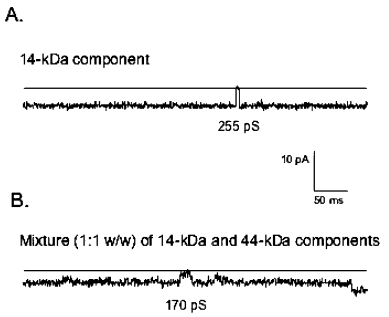

FIGURE 5: Typical single channel currents observed at pH 5.5 after addition of the 14-kDa component alone (A), or of the 1:1 (w/w) mixture of the two components of the PS149B1 binary crystal (B), to the PLB solution in the cis chamber of the PLB setup. The final protein concentration was 5−20 μg/mL. The single channel conductances determined at a −20 mV holding voltage are indicated under each current trace. Horizontal continuous lines indicate the estimated closed state of the channels.

the increase of the current noise following protein addition and by the occasional presence of current spikes of variable amplitude in the recordings (not shown). Therefore, ion channel activity of all recombinant proteins, either individually or in combination, was assessed under acidic pH conditions, i.e., in the PLB solution at pH 5.5. The 14-kDa protein alone did not partition easily into membranes compared to the PS149B1 toxin. The channels formed by the 14-kDa moiety (Figure 5A) had conductances ranging from 15 to approximately 300 pS (Table 2). They never displayed any flickering activity and were cation-selective, as demonstrated by a shift of about 15 mV toward negative voltages under 450:150 mM (cis:trans) KCl ionic gradient conditions (not shown). The 44-kDa protein alone did not insert easily into the PLBs, and clearly resolvable channels were rarely observed (not shown), even when the protein was reconstituted into liposomes which were subsequently fused to prepainted PLBs (13). The conductance of the 44-kDa channels ranged between 15 and 750 pS (Table 2). The 1:1 (w/w) mixture of the 14-kDa and the 44-kDa components, corresponding to a 3:1 molar ratio of the 14 to the 44 kDa, almost did not insert into PLBs. When it did, ion channels (Figure 5B) were observed with biophysical properties generally comparable to those of the 14-kDa component alone (not shown).

Current traces recorded from experiments in which the 40-kDa truncated product was used either alone or in combination with the 14-kDa component are shown in Figure 6. The 40-kDa protein inserted better than the 14- and the 44-kDa components of PS149B1 but not as efficiently as

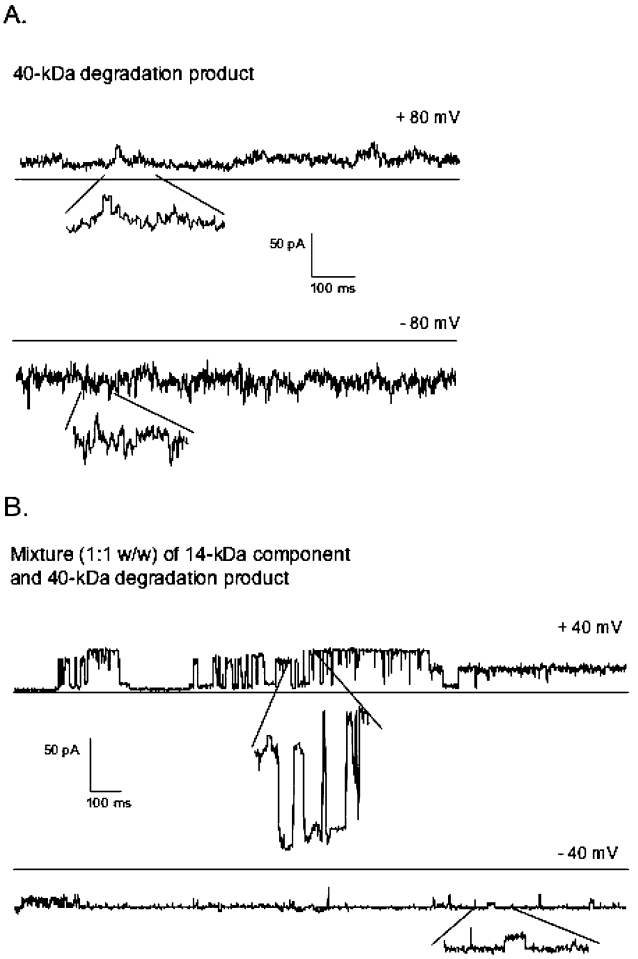

FIGURE 6: Single channel currents recorded in the PLB solution at pH 5.5 of the 40-kDa truncated product alone (A) and of the 1:1 (w/w) mixture of the 40-kDa and the 14-kDa proteins (B). Holding voltages are indicated over the current traces. Expanded time scale [by a factor of ∼3] and amplitude scale [by ∼2 in (A) and for the lower trace of (B) and by ∼4 for the upper trace of (A)] traces are shown under each main trace. Note that in (B) the channels were voltage-dependent; they tended to remain open in a low conductance state at −40 mV, while they were far more active at +40 mV. Horizontal continuous lines indicate the estimated closed state of the channels.

the PS149B1 binary toxin. It formed channels with conductances between 8 and 430 pS (Table 2) and occasional flickering activity. Figure 6A shows an example of the membrane-destabilizing effect of the 40-kDa protein: only poorly resolved channels could be observed in the recording. When a 3:1 molar mixture of the 14-kDa component and

the purified 40-kDa fragment was incubated overnight at 4 °C before being added to the PLB bath, ion channel activity was clearly observed (Figure 6B). Similar results were obtained by mixing the 14-kDa component of the binary toxin and the 40-kDa truncated product at the beginning of the experiment (not shown). Unlike the channel currents produced by the 14-kDa/44-kDa protein mixture, the observed electrical activity with the 14-kDa/40-kDa component mixture reflected that produced by the wild-type binary toxin rather than just its 14-kDa component alone (Table 2). While PS149B1, the native binary toxin, displayed the same kinetic behavior at positive and negative applied voltages, the reconstituted pair of the 14- and 40-kDa proteins displayed large, flickering channels at positive voltage only.

Interestingly, the channel currents of each individual component of the binary toxin returned to zero in at least half of the experiments, whereas the PS149B1 toxin and the 40-kDa truncated product channels tended to stay open in 60% and 67% of the cases, respectively. Moreover, the currents observed with the 3:1 molar mixture of the 14- and 40-kDa proteins returned to zero only in 9% of the experiments (Table 2).

DISCUSSION

The permeabilizing activity of PS149B1 toxin, a new binary crystal that kills western corn rootworm larvae, was investigated using large unilamellar vesicles and planar lipid bilayers. The native binary toxin as well as the 14-kDa or the 44-kDa recombinant proteins permeabilized LUVs. This permeabilization assay using the efflux of calcein, whose hydrated Stokes radius is 0.75 nm (*31*), suggested that the pores formed by the toxin in LUVs were at least 1.5 nm in diameter.

Under alkaline pH conditions, which are representative of the lepidopteran larval midgut environment, only membrane destabilization was observed in PLBs using either the native solubilized binary toxin, the recombinant Cry34Ab1 protein (14-kDa component), or the Cry35Ab1 protein (44-kDa component). However, at acidic pH, the solubilized binary toxin, the 14-kDa component, the 44-kDa component, and the 3:1 molar mixture of either the 14-kDa protein and the 44-kDa component or, alternatively, the 14-kDa component and 40-kDa truncated product of the 44-kDa component all formed ion channels in PLBs. The origin of this pH dependence is not clear. Since the isoelectric point of both proteins is acidic (pH 4.8 for the 44 kDa and pH 6.7 for the 14 kDa), the charge of the proteins at more extreme alkaline pHs would drastically affect their initial interactions with the planar lipid bilayer. Presumably, the surface charge in alkaline buffers is not favorable to proper membrane insertion to form a functional pore. The observed destabilization may be caused by improper surface orientation of the toxin to the membrane resulting in disorganized insertion. In any case, we considered that the channel conductances of the 14-kDa/44-kDa protein reconstituted mixture were principally due to the 14-kDa component only since the observed conductances mimicked those produced by this protein alone. The finding that membrane bioactivity was optimum at pH 5.5 is relevant because the environment in which the toxin becomes effective (i.e., the gut of the western corn rootworm larva) is likely acidic as is the case for other coleopterans (*32*). Therefore, the data strongly indicate that the PS149B1 binary toxin and the mixture of its components act as pore-forming toxins with a mode of action that appears to be similar, at the in vitro membrane level, to that of other *B. thuringiensis* toxins (*1*, *14*, *15*, *24*, *33*−*36*), *B. sphaericus* toxins (*6*), and several other bacterial toxins (*37*, *38*). Our data suggest that, like other *B. thuringiensis* and *B. sphaericus* toxins, the PS149B1 binary toxin increases the permeability of the plasma membrane of midgut epithelial cells in susceptible corn rootworm larvae, leading to eventual larval death (*19*). However, relative to our understanding of the mode of action of other *B. thuringiensis* and *B. sphaericus* toxins, the exact mechanism by which PS149B1 causes membrane permeabilization in vivo remains unknown.

Interestingly, the channels formed by PS149B1 and by the 3:1 mixture of its two components had the largest conductances, compared to those of the channels of the 14-kDa component and the 40-kDa truncated product of the 44-kDa component of the toxin (Table 2). Furthermore, the PS149B1 channels and those made by the 14-kDa/40-kDa protein mixture tended to remain much more in the open state than the channels formed by the individual moieties of the binary toxin (Table 2). Taken together, these observations suggest that the efficacy of the toxin results from the capacity of its two components to insert together into biological membranes and form large channels which do not close very often. This, of course, would ensure an efficient permeabilizing effect responsible for the target insect's death.

Planar lipid experiments provided direct evidence for ion channel formation by the PS149B1 toxin and its components under appropriate experimental conditions, although it cannot totally be excluded that permeabilization may have occurred as a result of membrane disruption by the proteins, i.e., without formation of structurally organized pores. As both phospholipid vesicles and planar lipid bilayers are missing specific PS149B1 toxin receptors normally present in sensitive epithelial target cells, it is possible that under our experimental conditions protein insertion and pore assembly may have been rare events, similar to what was reported with other *B. thuringiensis* toxins (*14*, *15*, *24*, *34*, *35*) where receptor reconstitution in bilayers resulted in a significant increase in pore-forming efficacy (*13*).

Once it was determined that solubilized binary toxin could form ion channels such as other known Cry1 toxins, it was of interest to assess the roles of the two individual components. The difficulties encountered in inserting the 44-kDa recombinant protein into PLBs combined with the appearance of a smaller, more stable 40-kDa truncated product suggested that the latter may be implicated in ion channel formation. Alone, the 40-kDa truncated product inserted in PLBs with greater ease than the 44-kDa component, but the conductance of the channels is smaller than that of PS149B1. However, when the 14-kDa moiety was added to the PLB chamber, ion channels were formed that displayed conductances and kinetic properties similar to those observed with the full toxin. This suggests that proteolytic activation of the 44-kDa protein may be important for the full activity of the PS149B1 toxin on sensitive cells (*19*). Although the cysteine protease papain was used to assess toxin sensitivity, a recent publication by Bown et al. (*39*) suggests that the major digestive cysteine proteases in Diabrotica larvae are cathepsin B and L-like proteinases. The poor success rate with the

solubilized 44k-Da protein in producing defined ion channels lends further support to the notion that this purified protein is not the active form of this component of the PS149B1 toxin. This poor activity could be partially explained by the protein's highly aggregated state, rendering membrane integration difficult. However, some channel activity was actually recorded with this protein, suggesting that since the 44-kDa protein could not be purified without the presence of some 40-kDa truncated product due to spontaneous activation, the observed activity may be due to the presence of the 40-kDa protein rather than the 44-kDa component of the binary toxin.

It should be noted that calcium-free solutions were used in the calcein efflux experiments whereas 1 mM calcium was used in the PLB baths. It cannot be completely excluded, therefore, that calcium may have played a role in permeabilization and channel formation by PS149B1 and its two moieties, depending on the experimental approach. However, there is no reported evidence for such a role for any Bt toxins studied so far.

The exact mode of action of PS149B1 binary toxin remains to be elucidated. Interestingly, whereas no homology could be revealed between the toxin's components and any known *B. thuringiensis* toxin sequence, its 44-kDa moiety shares some resemblance with the mosquitocidal binary toxin components of *B. sphaericus* (*19*), which may suggest a common mode of action between the two. Indeed, with the combination of our data and the toxicity results of Herman et al. (*20*), some similarities between the *B. thuringiensis* and *B. sphaericus* binary toxins are beginning to emerge. It was proposed that the membrane permeabilization effect of *B. sphaericus* toxins could be explained by the fact that its BinA component displayed the best pore-forming ability, whereas its BinB component facilitated pore formation by BinA (*6*). This was in agreement with data showing that BinB promoted the specific binding of BinA to gut brush border membranes prepared from *Culex pipiens* larvae (*40*, *41*). At high concentrations, BinA, but not BinB, was toxic to *C. pipiens* larvae (*42*−*44*), while the presence of BinB was required for BinA's full activity (*45*). BinB may thus assist the partition of BinA into the membrane. Similar to the Bin toxins, only one component of the PS149B1 binary toxin (i.e., the 14-kDa protein) was toxic to the corn rootworm larvae. Although the 44-kDa component was nontoxic, its addition to 14-kDa component was synergistic and was required to achieve maximal toxicity (*20*). The observation that both BinA and BinB formed pores in PLBs, though with quite different efficiencies, was consistent with the fact that both proteins possess two homologous hydrophobic regions which could be involved in membrane insertion and pore formation (*21*). While the present work demonstrated that the best permeabilization effect of PS149B1 was achieved with the full toxin or the mixture of its moieties, it did not clearly establish, as was shown in the case of the *B. sphaericus* binary toxins, which of the two components of the PS149B1 toxin was principally responsible for pore formation and whether one of them had to insert first into the membrane to facilitate the permeabilizing effect of the toxin. As shown in Table 2, the 40-kDa truncated product was approximately 2-fold easier to incorporate successfully into PLBs than the 14-kDa component and, in combination with the latter, was roughly 3-fold more efficient in ion channel formation, reaching 72% of native PS149B1 capacity to form detectable channels in PLBs.

Several important issues remain to be addressed to elucidate the mode of action of the PS149B1 toxin further. The activation, degradation, and aggregation patterns of its two moieties under physiological conditions need to be characterized in greater detail, and whether oligomerization of the toxin takes place before or after insertion into the membrane remains to be determined. More work is needed to study precisely the process of pore formation and determine the biophysical properties of the functional pores. In view of the membrane-destabilizing abilities demonstrated by each of the individual components, other permeabilization mechanisms, e.g., detergent effects and the induction of membrane defects, should be considered.

In conclusion, this study clearly demonstrates that the novel PS149B1 toxin from *B. thuringiensis* is a pore-forming toxin in artificial phospholipid membranes. Results from these experiments suggest that the binary toxin manifests its coleopteran larvicidal activity from its capacity to permeabilize target cell membranes in a way that may be similar to the mechanism of action of other nonbinary *B. thuringiensis* toxins and of binary *B. sphaericus* toxins.

ACKNOWLEDGMENT

The authors thank J. Russell (Dow AgroSciences, San Diego, CA) for the production of the different native or recombinant crystal preparations used in this study and T. S. Dhadialla and K. Narva (Dow AgroSciences, Indianapolis, IN) and A. Abad and R. Hermann (Pioneer Hi-Bred, Johnston, IA) for stimulating discussions.

REFERENCES

1. Schnepf, E., Crickmore, N., van Rie, J., Lereclus, D., Baum, J., Feitelson, J., Zeigler, D. R., and Dean, D. H. (1998) *Bacillus thuringiensis* and its pesticidal crystal proteins, *Microbiol. Mol. Biol. Rev. 62*, 775−806.
2. Crickmore, N., Zeigler, D. R., Feitelson, J., Schnepf, E., van Rie, J., Lereclus, D., Baum, J., and Dean, D. H. (1998) Revision of the nomenclature for the *Bacillus thuringiensis* pesticidal crystal proteins, *Microbiol. Mol. Biol. Rev. 62*, 807−813.
3. Feitelson, J. S., Payne, J., and Kim, L. (1992) *Bacillus thuringiensis*: Insects and beyond, *Bio/Technology 10*, 271−275.
4. Siegel, J. P. (2001) The mammalian safety of *Bacillus thuringiensis*-based insecticides, *J. Invertebr. Pathol. 77*, 13−21.
5. Charles, J. F., Nielsen-LeRoux, C., and Delécluse, A. (1996) *Bacillus sphaericus* toxins: Molecular biology and mode of action, *Annu. Rev. Entomol. 41*, 451−472.
6. Schwartz, J. L., Potvin, L., Coux, F., Charles, J. F., Berry, C., Humphreys, M. J., Jones, A. F., Bernhart, I., Dalla Serra, M., and Menestrina, G. (2001) Permeabilization of model lipid membranes by *Bacillus sphaericus* mosquitocidal binary toxin and its individual components, *J. Membr. Biol. 184*, 171−183.
7. Masson, L., Lu, Y. J., Mazza, A., Brousseau, R., and Adang, M. J. (1995) The CryIA(c) receptor purified from *Manduca sexta* displays multiple specificities, *J. Biol. Chem. 270*, 20309−20315.
8. Masson, L., Mazza, A., and De Crescenzo, G. (2000) Interactions of bacterial protein toxins with their purified soluble insect receptor, in *Methods in Molecular Biology* (Walker, J. M., Ed.) pp 189−201, Humana Press, Totowa, NJ.
9. van Rie, J., Jansens, S., Höfte, H., Degheele, D., and Van Mellaert, H. (1989) Specificity of *Bacillus thuringiensis* delta-endotoxins. Importance of specific receptors on the brush border membrane of the mid-gut of target insects, *Eur. J. Biochem. 186*, 239−247.
10. van Rie, J., Jansens, S., Höfte, H., Degheele, D., and Van Mellaert, H. (1990) Receptors on the brush border membrane of the insect midgut as determinants of the specificity of *Bacillus thuringiensis* delta-endotoxins, *Appl. Environ. Microbiol. 56*, 1378−1385.

11. Schwartz, J. L., Juteau, M., Grochulski, P., Cygler, M., Préfontaine, G., Brousseau, R., and Masson, L. (1997) Restriction of intramolecular movements within the Cry1Aa toxin molecule of *Bacillus thuringiensis* through disulfide bond engineering, *FEBS Lett. 410*, 397−402.
12. Schwartz, J. L., and Masson, L. (2000) Structure−function analysis of cysteine-engineered entomopathogenic toxins, in *Bacterial Toxins: Methods And Protocols* (Holst, O., Ed.) pp 101−113, Humana Press, Totowa, NJ.
13. Schwartz, J. L., Lu, Y. J., Söhnlein, P., Brousseau, R., Laprade, R., Masson, L., and Adang, M. J. (1997) Ion channels formed in planar lipid bilayers by *Bacillus thuringiensis* toxins in the presence of *Manduca sexta* midgut receptors, *FEBS Lett. 412*, 270−276.
14. Schwartz, J. L., Garneau, L., Savaria, D., Masson, L., Brousseau, R., and Rousseau, E. (1993) Lepidopteran-specific crystal toxins from *Bacillus thuringiensis* form cation- and anion-selective channels in planar lipid bilayers, *J. Membr. Biol. 132*, 53−62.
15. Slatin, S. L., Abrams, C. K., and English, L. (1990) Delta-endotoxins form cation-selective channels in planar lipid bilayers, *Biochem. Biophys. Res. Commun. 169*, 765−772.
16. Gazit, E., LaRocca, P., Sansom, M. S. P., and Shai, Y. (1998) The structure and organization within the membrane of the helices composing the pore-forming domain of *Bacillus thuringiensis* delta-endotoxin are consistent with an "umbrella-like" structure of the pore, *Proc. Natl. Acad. Sci. U.S.A. 95*, 12289−12294.
17. Masson, L., Tabashnik, B. E., Liu, Y. B., Brousseau, R., and Schwartz, J. L. (1999) Helix 4 of the *Bacillus thuringiensis* Cry1Aa toxin lines the lumen of the ion channel, *J. Biol. Chem. 274*, 31996−32000.
18. Knowles, B. H., and Ellar, D. J. (1987) Colloid-osmotic lysis is a general feature of the mechanism of action of *Bacillus thuringiensis* δ-endotoxins with different insect specificity, *Biochim. Biophys. Acta 924*, 509−518.
19. Moellenbeck, D. J., Peters, M. L., Bing, J. W., Rouse, J. R., Higgins, L. S., Sims, L., Nevshemal, T., Marshall, L., Ellis, R. T., Bystrak, P. G., Lang, B. A., Stewart, J. L., Kouba, K., Sondag, V., Gustafson, V., Nour, K., Xu, D. P., Swenson, J., Zhang, J., Czapla, T., Schwab, G., Jayne, S., Stockhoff, B. A., Narva, K., Schnepf, H. E., Stelman, S. J., Poutre, C., Koziel, M., and Duck, N. (2001) Insecticidal proteins from *Bacillus thuringiensis* protect corn from corn rootworms, *Nat. Biotechnol. 19*, 668−672.
20. Herman, R. A., Scherer, P. N., Young, D. L., Mihaliak, C. A., Meade, T., Woodsworth, A. T., Stockhoff, B. A., and Narva, K. E. (2002) Binary insecticidal crystal protein from *Bacillus thuringiensis*, strain PS149B1: Effects of individual protein components and mixtures in laboratory bioassays, *J. Econ. Entomol. 95*, 635−639.
21. Baumann, P., Clark, M. A., Baumann, L., and Broadwell, A. H. (1991) *Bacillus sphaericus* as a mosquito pathogen: properties of the organism and its toxins, *Microbiol. Rev. 55*, 425−436.
22. Morse, R. J., Yamamoto, T., and Stroud, R. M. (2001) Structure of Cry2Aa suggests an unexpected receptor binding epitope, *Structure 9*, 409−417.
23. Li, J. D., Carroll, J., and Ellar, D. J. (1991) Crystal structure of insecticidal delta-endotoxin from *Bacillus thuringiensis* at 2.5 Å resolution, *Nature 353*, 815−821.
24. Grochulski, P., Masson, L., Borisova, S., Pusztai-Carey, M., Schwartz, J. L., Brousseau, R., and Cygler, M. (1995) *Bacillus thuringiensis* CryIA(a) insecticidal toxin: crystal structure and channel formation, *J. Mol. Biol. 254*, 447−464.
25. Galitsky, N., Cody, V., Wojtczak, A., Ghosh, D., Luft, J. R., Pangborn, W., and English, L. (2001) Structure of the insecticidal bacterial delta-endotoxin Cry3Bb1 of *Bacillus thuringiensis*, *Acta Crystallogr., Sect. D: Biol. Crystallogr. 8*, 1101−1109.
26. Ellis, R. T., Stockhoff, B. A., Stamp, L., Schnepf, H. E., Schwab, G. E., Knuth, M., Russell, J., Cardineau, G. A., and Narva, K. E. (2002) Novel *Bacillus thuringiensis* binary insecticidal crystal proteins active on western corn rootworm, *Diabrotica virgifera virgifera* LeConte, *Appl. Environ. Microbiol. 68*, 1137−1145.
27. MacDonald, R. C., MacDonald, R. I., Menco, B. P. M., Takeshita, K., Subbarao, N. K., and Hu, L. (1991) Small-volume extrusion apparatus for preparation of large, unilamellar vesicles, *Biochim. Biophys. Acta 1061*, 297−303.
28. Benachir, T., and Lafleur, M. (1995) Study of vesicle leakage induced by melittin, *Biochim. Biophys. Acta 1235*, 452−460.
29. Müller, P., Rudin, D. O., Tein, H. T., and Wescott, W. C. (1963) Methods for formation of single bimolecular lipid membranes in aqueous solution, *J. Phys. Chem. 67*, 534−535.
30. Cohen, F. S. (1986) Fusion of liposomes to planar bilayers, in *Ion channel reconstitution* (Miller, C., Ed.) pp 131−139, Plenum Press, New York.
31. Yoshida, N., Tamura, M., and Kinjo, M. (2000) Fluorescence correlation spectroscopy: a new tool for probing the microenvironment of the internal space of organelles, *Single Mol. 1*, 279−283.
32. Koller, C. N., Bauer, L. S., and Hollingworth, R. M. (1992) Characterization of the pH-mediated solubility of *Bacillus thuringiensis* var. *san diego* native δ-endotoxin crystals, *Biochem. Biophys. Res. Commun. 184*, 692−699.
33. English, L., and Slatin, S. L. (1992) Mode of action of delta-endotoxins from *Bacillus thuringiensis*: a comparison with other bacterial toxins, *Insect Biochem. Mol. Biol. 22*, 1−7.
34. Knowles, B. H., Blatt, M. R., Tester, M., Horsnell, J. M., Carroll, J., Menestrina, G., and Ellar, D. J. (1989) A cytolytic delta-endotoxin from *Bacillus thuringiensis* var. *israelensis* forms cation-selective channels in planar lipid bilayers, *FEBS Lett. 1989 244*, 259−262.
35. Lorence, A., Darszon, A., Díaz, C., Liévano, A., Quintero, R., and Bravo, A. (1995) Delta-endotoxins induce cation channels in *Spodoptera frugiperda* brush border membranes in suspension and in planar lipid bilayers, *FEBS Lett 360*, 217−222.
36. Schwartz, J. L., and Laprade, R. (2000) *Bacillus thuringiensis* toxins: membrane permeabilization and pore formation, in *Entomopathogenic Bacteria: from Laboratory to Field Application* (Charles, J.-F., Delécluse, A., and Nielsen-LeRoux, C., Eds.) pp 199−219, Kluwer Associate Publishing, Norwell, MA.
37. Menestrina, G., and Vécsey-Semjén, B. (1999) Biophysical methods and model membranes for the study of bacterial pore-forming toxins, in *The comprehensive sourcebook of bacterial protein toxins* (Alouf, J. E., and Freer, J. H., Eds.) pp 287−309, Academic Press, London.
38. Harvey, A. L. (1990) Cytolytic toxins, in *Handbook of toxinology*, pp 1−66, Marcel Dekker, New York.
39. Bown, D. P., Wilkinson, H. S., Jongsma, M. A., and Gatehouse, J. A. (2004) Characterisation of cysteine proteases responsible for digestive proteolysis in guts of larval Western corn rootworm (*Diabrotica virgifera*) by expression in the yeast *Pichia pastoris*, *Insect Biochem. Mol. Biol. 34*, 305−320.
40. Oei, C., Hindley, J., and Berry, C. (1992) Binding of purified *Bacillus sphaericus* binary toxin and its deletion derivatives to *Culex quinquefasciatus* gut: elucidation of functional binding domains, *J. Gen. Microbiol. 138*, 1515−1526.
41. Charles, J. F., Silva, M. H., NielsenLeRoux, C., Humphreys, M. J., and Berry, C. (1997) Binding of the 51- and 42-kDa individual components from the *Bacillus sphaericus* crystal toxin to mosquito larval midgut membranes from *Culex* and *Anopheles* sp. (Diptera: Culicidae), *FEMS Microbiol. Lett. 156*, 153−159.
42. Broadwell, A. H., Baumann, L., and Baumann, P. (1990) Larvicidal properties of the 42 and 51 kilodalton *Bacillus sphaericus* proteins expressed in different bacterial hosts: evidence for a binary toxin, *Curr. Microbiol. 21*, 361−366.
43. De la Torre, F., Bennardo, T., Sebo, P., and Szulmajster, J. (1989) On the respective roles of the two proteins encoded by the *Bacillus sphaericus* 1593M toxin genes expressed in *Escherichia coli* and *Bacillus subtilis*, *Biochem. Biophys. Res. Commun. 164*, 1417−1422.
44. Nicolas, L., Nielsen-LeRoux, C., Charles, J.-F., and Delécluse, A. (1993) Respective role of the 42- and 51-kDa components of the *Bacillus sphaericus* toxin overexpressed in *Bacillus thuringiensis*, *FEMS Microbiol. Lett. 106*, 275−280.
45. Broadwell, A. H., Clark, M. A., Baumann, L., and Baumann, P. (1990) Construction by site-directed mutagenesis of a 39-kilodalton mosquitocidal protein similar to the larva-processed toxin of *Bacillus sphaericus* 2362, *J. Bacteriol. 172*, 4032−4036.

BI048946Z